Plasmon Resonance Spectroscopy of Gold-in-Gallium Oxide Peapod and Core/Shell Nanowires

Yi-Jen Wu, Chin-Hua Hsieh, Po-Ham Chen, Jing-Yang Li, Li-Jen Chou,* and Lih-Juann Chen*

Department of Materials Science and Engineering, National Tsing Hua University, No. 101, Section 2, Kuang-Fu Road, Hsinchu 30013, Taiwan

ARTICLE

ABSTRACT Light-scattering properties of individual gold-in-Ga_2O_3 peapod nanowires and gold-in-Ga_2O_3 core/shell nanowires were investigated by optical dark-field microscopy. The observed scattering peaks are suggested to result from plasmonic resonance of the gold nanopeas and nanorods in the Ga_2O_3 nanowires. As the diameter of gold peapod increases, the resonance peak of the optical scattering spectra showed a red-shift. In addition, as the gold peas are elongated along one axis, the corresponding plasmon resonance peak splits into two peaks at shorter and longer wavelengths. The cladding Ga_2O_3 dielectric layer also plays a key role in light-scattering behavior. The observed modulation in the p-polarized spectrum revealed that future vertical nanoplasmonic devices made by plasmonic nanocavity due to the short propagation length of surface plasmons can be realized and optimized.

KEYWORDS: light scattering · surface plasmon (SP) · gold-in-Ga_2O_3 peapod nanowires · gold-in-Ga_2O_3 core/shell nanowires

In recent years, metal nanoparticles and complex nanostructures have attracted significant attention because of their versatile application as highly efficient chemical or biological sensors,[1,2,5] molecular rulers,[3] waveguides,[4−6] photonic circuits,[7] and nanophotonic devices,[8,9] or even for their aesthetic appeal in stained glass. These applications are primarily based on the exceptional optical properties of metals when plasmons are excited in the bulk or on the surface.[10−12] When the incident photon frequency is resonant with the coherent oscillation of the conduction electrons in the subwavelength metal nanoparticles, surface plasmons (SPs) can be excited and radiate at a frequency which results in a unique color not present in the bulk metal. This phenomenon is known as localized surface plasmon resonance (LSPR), or particle plasmons,[11−13] and it is due to the charge density oscillation and confinement between the metal nanoparticles, if the particle size is significantly smaller than the wavelength of incident light. As localized surface plasmons (LSPs) are excited, intense light absorption, light scattering, and local electromagnetic field enhancement of the metal particle occur. The features strongly depend on a particle's composition, size, shape, and local dielectric environment. For particles with a spherical symmetry, Mie scattering theory provides a rigorous solution that describes well the optical spectra of spheres of any size. For particles with nonspherical geometries, Gans theory proposes that the extinction, scattering, and absorption of light depend on the aspect ratio of particles but not on the actual dimensions. Both Mie theory and Gans theory can be applied to investigate optical properties of metallic nanoparticles much smaller than the wavelength of incident light. If the surrounding electric field of the particle is considered a constant, the interaction between incident light and the particle is governed by electrostatics and can be taken as quasistatic approximation. In addition, each particle is considered to scatter independently and not experience interference from wave scattering by adjacent particles.

However, when two metal nanoparticles are brought within 2.5 times the particle diameter of one another, distance between the two particles will have a significant impact on their plasmonic behaviors. This phenomenon, in which the electric charge distribution of the nearby particle results in an additional force greater than the externally applied electromagnetic field, is known as electromagnetic field coupling.[14−18] In this case amendments to Mie and Gans theory are necessary. The effect of near-field optical coupling can be verified theoretically and experimentally. As interparticle distance decreases, the

*Address correspondence to ljchou@mx.nthu.edu.tw, ljchen@mx.nthu.edu.tw.

Received for review August 20, 2009 and accepted February 02, 2010.

Published online February 11, 2010.
10.1021/nn901044t

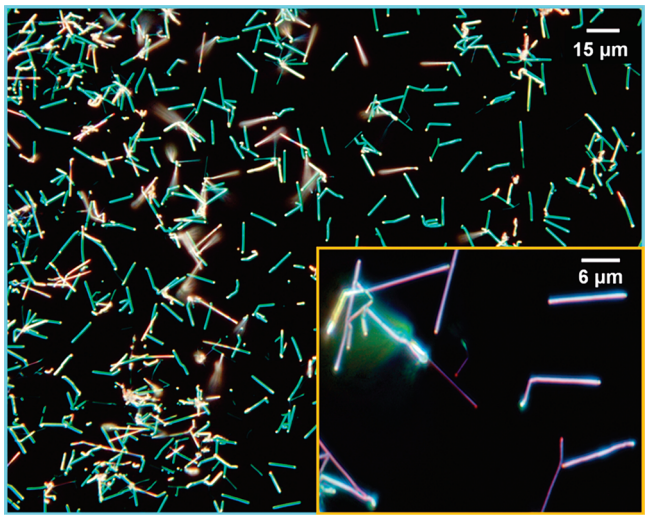

Figure 1. Dark-field light-scattering image of the free-standing as-grown pure Ga_2O_3 nanowires and gold-in-Ga_2O_3 complex nanowires on a SiO_2 substrate. Inset shows a magnified view of the image.

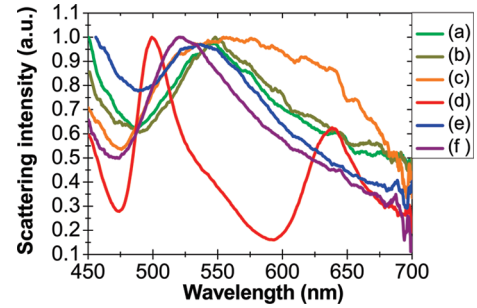

Figure 2. Normalized light-scattering spectra from various nanowires on SiO_2 substrate; a gold-in-Ga_2O_3 peapod nanowire with the gold-pea diameter of (a) 40, (b) 50, and (c) 80 nm, (d) a gold-in-Ga_2O_3 of ellipsoidal peapod nanowire, the average aspect ratio of gold nanorod is 3.8; (e) a gold-in-Ga_2O_3 core/shell nanowire with core diameter of 20 nm and (f) a pure Ga_2O_3 nanowire.

wavelength of the resonance peak is red-shifted compared to the peak of an isolated single particle under the incident light parallel to the axial direction; while a blue-shift of the peak is observed under incident light perpendicular to the axial direction.[16−18] On the other hand, as interparticle distance becomes greater than 2.5 times the particle diameter, the coupling effect becomes negligible and the surrounding field of the particles in this condition is considered decoupled and independent.[14−18]

In contrast to previous top-down nanolithographic techniques,[16−20] such as electron-beam lithography and on-wire lithography, single-crystalline gold-in-Ga_2O_3 peapod nanowires and gold-in-Ga_2O_3 core/shell nanowires were grown by a bottom-up method. The diameters and interparticle distance of gold peas, and/or the length and core diameters of gold rods, were tuned during growth in a controlled manner, and the plasmon resonances of these nanostructures were systematically investigated. The pronounced photoresponse of a single gold-in-Ga_2O_3 peapod nanowire under the illumination of 532 nm laser light is attributed to the surface plasmon resonance effect of the inner embedded Au peas. Further investigations of the localized surface plasmon resonance effect for gold nanoparticles in the Ga_2O_3 nanowire matrix were also carried out. These results are expected to be crucial to optimization of performance and in future nanoplasmonic devices.

RESULTS AND DISCUSSION

Scattering Spectra from Single Nanowire. Figure 1 is the optical dark-field image of the as-grown gold-in-Ga_2O_3 nanowires; an enlarged image is shown in the lower right-hand inset. A clear contrast image of the stimulated nanowires was obtained, after suppressing the incident light. The results indicate that uniformly distributed nanowires can be easily and quickly identified by this optical technique. Figure 2 shows the light-scattering spectra from different gold-in-Ga_2O_3 peapod nanowires with varying gold pea diameters, a gold-in-Ga_2O_3 core/shell nanowire, and a pure Ga_2O_3 nanowire. In Figure 2a, the gold pea diameter is 40 nm and the plasmon resonance peak is located at 545 nm; as the diameter of gold pea is increased to 50 and 80 nm by the postannealing process, the resonance peaks of the nanowires are red-shifted to 548 nm (Figure 2b) and 573 nm (Figure 2c), respectively. In addition, as the gold peas are elongated in one axis and become ellipsoid or even rodlike in shape, the corresponding plasmon resonance spectrum exhibits two distinct peaks at shorter (499 nm) and longer (638 nm) wavelengths, as shown in Figure 2d. As the peas are continuously elongated to the ends, effectively forming a core/shell (gold-in-Ga_2O_3) nanowire, the corresponding peak (for a core diameter of 20 nm) is at 537 nm as shown in Figure 2e. Note that the peaks of gold-in-Ga_2O_3 peapod and gold-in-Ga_2O_3 core/shell nanowires are remarkably red-shifted compared to that of pure Ga_2O_3 nanowire (Figure 2f). These results imply that the inner embedded gold nanostructure is a key factor in the light-scattering behavior of complex gold-in-Ga_2O_3 nanowires. (Figure 1 in the supporting file shows the SEM images of the microstructures of the actual nanowires studied in the scattering spectra of Figure 2.)

Mie Theory. To further investigate the LSPR effect of Au nanopeas in the Ga_2O_3 nanowires, such as the optimum extinction and scattering and absorption efficiencies corresponding to different nanopea diameters, theoretical calculations based on Mie theory with some modifications were applied. According to Mie's equations, the extinction coefficient, scattering coefficient, and absorption coefficient for a collection of independent spherical particles are given by eqs 1−3:[21]

$$\frac{\gamma_{ext}}{NV} = \frac{3\pi\varepsilon_{med}^{3/2}}{\lambda a^3}\sum_{L=1}^{\infty}(2L+1)Re(A_L + B_L) \qquad (1)$$

$$\frac{\gamma_{sca}}{NV} = \frac{3\pi\varepsilon_{med}^{1/2}}{\lambda a^3}\sum_{L=1}^{\infty}(2L+1)(|A_L|^2 + |B_L|^2) \quad (2)$$

$$\gamma_{abs} = \gamma_{ext} - \gamma_{sca} \quad (3)$$

where $a = 2\pi R\varepsilon_{med}^{1/2}/\lambda$ and R is the radius of the spheres, V is the volume of the spheres ($=^4/_3\pi R^3$), λ is the wavelength of light in a vacuum, ε_{med} is the dielectric constant of the surrounding medium, and N is the number of spheres per unit volume. L indicates the L^{th} electric and magnetic partial oscillations of the electromagnetic field inside the sphere. The coefficients A_L and B_L are the first and second kind of spherical Bessel functions of the complex dielectric constant of the sphere.

To simplify the calculations, we consider the incident light a plane wave, and gold nanopeas perfect spheres with average diameters of 20, 30, 40, 50, 60, 70, or 80 nm, although the actual interparticle distances of the Au peas fluctuate notably, ranging from 40 to 200 nm. The coupling effect is assumed to be negligible and the wave scattering of each gold sphere to be independent. The effective dielectric constant of the surrounding medium should be between that of air ($n_{air} = 1$) and the Ga_2O_3 cladding matrix ($n_{Ga_2O_3} = 1.8$).[22] Assuming $n_{med} = 1.4$ ($\varepsilon_{med} = n_{med}^2$), ε_{med} is equal to 1.96. The scattering efficiencies corresponding to different Au diameters from Mie's theory are presented in Figure 3. The maximum peaks of simulated efficiencies illustrated in Figure 3 agree well with the light-scattering peaks in Figure 2 (Table 1). The absorption peak at 532 nm for gold peas with an average diameter of 40 nm embedded in the Ga_2O_3 nanowires was also identified. It is suggested that the LSPR effect is the dominant factor in the enhanced photoresponse of nanophotonic switches based on gold-in-Ga_2O_3 peapod nanowire. (Figure 2 and Figure 3 in the Supporting Information).

Gans Theory. For pronounced split resonance peaks from the elongated gold nanopeas embedded in the Ga_2O_3 matrix, the optimum extinction, scattering, and absorption efficiencies for different aspect ratios of Au ellipsoids were calculated adopting Gans theory with similar assumptions. The Gans modifications of Mie's theory for elongated spheroids within the dipole approximations assume that the absorption of incident energy is mainly caused by electric dipole oscillation of the nanoparticles. The extinction coefficient, scattering coefficient, and thus absorption coefficient of small prolate particles in homogeneous medium are given by eqs 4−6:[21]

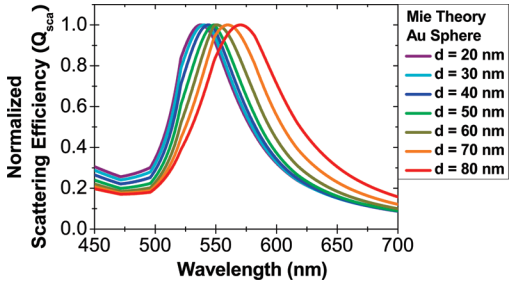

Figure 3. Calculated scattering efficiencies for gold nanospheres with diameters of 20, 30, 40, 50, 60, 70, and 80 nm, embedded in the mix dielectric medium of Ga_2O_3 matrix and air ($n_{med} = 1.4$), respectively.

TABLE 1. Comparisons between Experimental and Calculated Data

Au pea diameter (nm)	experimental plasmon peak (nm)	calculated plasmon peak (nm) by Mie theory
20	537	537.7
40	545	543.8
50	548	548.6
80	573	570.2

Au pea aspect ratio	experimental plasmon peaks (nm)	calculated plasmon peaks (nm) by Gans theory
3.8	499, 638	522, 635

$$\frac{\gamma_{ext}}{NV} = \frac{2\pi\varepsilon_{med}^{3/2}}{3\lambda}\sum_j \frac{\left(\frac{1}{P_j^2}\right)\varepsilon_i}{\left(\varepsilon_r + \frac{1-P_j}{P_j}\varepsilon_{med}\right)^2 + \varepsilon_i^2} \quad (4)$$

$$\frac{\gamma_{sca}}{NV} = \frac{8\pi^3 V\varepsilon_{med}^2}{3\lambda^4}\sum_j \frac{\left(\frac{1}{P_j^2}\right)[(\varepsilon_r - \varepsilon_{med})^2 + \varepsilon_i^2]}{\left(\varepsilon_r + \frac{1-P_j}{P_j}\varepsilon_{med}\right)^2 + \varepsilon_i^2} \quad (5)$$

$$\gamma_{abs} = \gamma_{ext} - \gamma_{sca} \quad (6)$$

where ε_r and ε_i are the real and imaginary parts of the material dielectric function of the particle, $\varepsilon_{particle}(\omega) = \varepsilon_r(\omega) + i\varepsilon_i(\omega)$, and $\varepsilon^{1/2} = n + i\kappa$. P_j are the depolarization factors of the three axes A, B, and C of the elongated ellipsoid with $A > B = C$, defined as eqs 7−9:[21,23,24]

$$P_A = \frac{1-e^2}{e^2}\left[\frac{e}{2}\ln\left(\frac{1+e}{1-e} - 1\right)\right] \quad (7)$$

$$P_B = P_C = \frac{1-P_A}{2} \quad (8)$$

$$e = \sqrt{1 - \left(\frac{B}{A}\right)^2} \quad (9)$$

The elongated gold nanopea is assumed to be an idealized ellipsoid, and the core diameter of the gold nanorod is assumed to be 40 nm. The effective dielectric constant of the surrounding medium is also assumed to be $\varepsilon_{med} = 1.96$ (corresponding to $n_{med} = 1.4$). We have adopted the optical constants for gold nanoparticles reported by Johnson and Christy.[25] Simulations for Au ellipsoids with aspect ratios of 3.0, 3.5, 3.8, and 4.0 are presented in Figure 4. The trend of red-shift of the peak with increasing Au aspect ratio is pronounced.

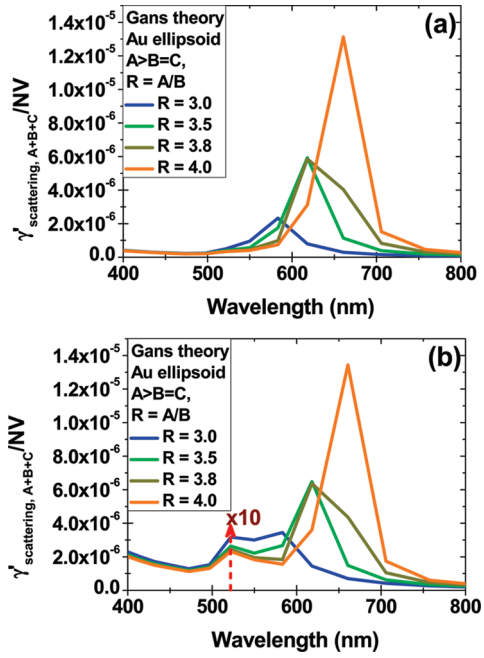

Figure 4. (a) Calculated scattering efficiencies for elongated gold nanopeas embedded in the Ga_2O_3 nanowire with aspect ratios in 3.0, 3.5, 3.8, and 4.0. (b) The intensity of scattering from short axes (B or C) of the gold ellipsoid is increased by one order than for that in panel a for better comparison.

The calculated maximum efficiencies in Figure 4 match the light scattering of a gold-in-Ga_2O_3 ellipsoidal peapod nanowire in Figure 2d, in which the average aspect ratio of gold peas is approximately 3.8 (Table 1). Hence, we suggest that the observed split scattering peaks represent the transverse and longitudinal plasmon resonance modes along the minor and major axes of gold ellipsoidal peas in the Ga_2O_3 nanowires.

Interference Phenomena in Scattering Spectra. To investigate the surface-plasmon-mediated optical interference phenomena of gold-in-Ga_2O_3 nanowires, a single peapod nanowire was excited by depolarized white light, and the perpendicular-oriented polarized (s-polarized) and parallel-oriented polarized (p-polarized) scattering light collected from the end of the nanowire. Surface plasmons were excited, bound, and propagated along the principal axis of the nanowire in a controlled direction accompanied by longitudinal fluctuations of surface charge density. A measured optical scattering spectrum with prominent modulation is observed, as shown in Figure 5 for a gold-in-Ga_2O_3 nanowire. In a comparison of the scattering spectra, excitation by p-polarized light results in pronounced modulation over the entire spectral range from 400 to 750 nm (Figure 5c); while excitation by s-polarized light does not (Figure 5d). We infer that the peapod nanostructure can be used as an optical Fabry–Pérot-type plasmon resonator along the longitudinal axis[26–29] (see Supporting Information). The results also indicate that SP waves excited by white light induce optical interference phenomena.

CONCLUSIONS

Gold-in-Ga_2O_3 peapod and core/shell nanowires may be synthesized in a controllable manner by carefully adjusting the growth parameters to tune

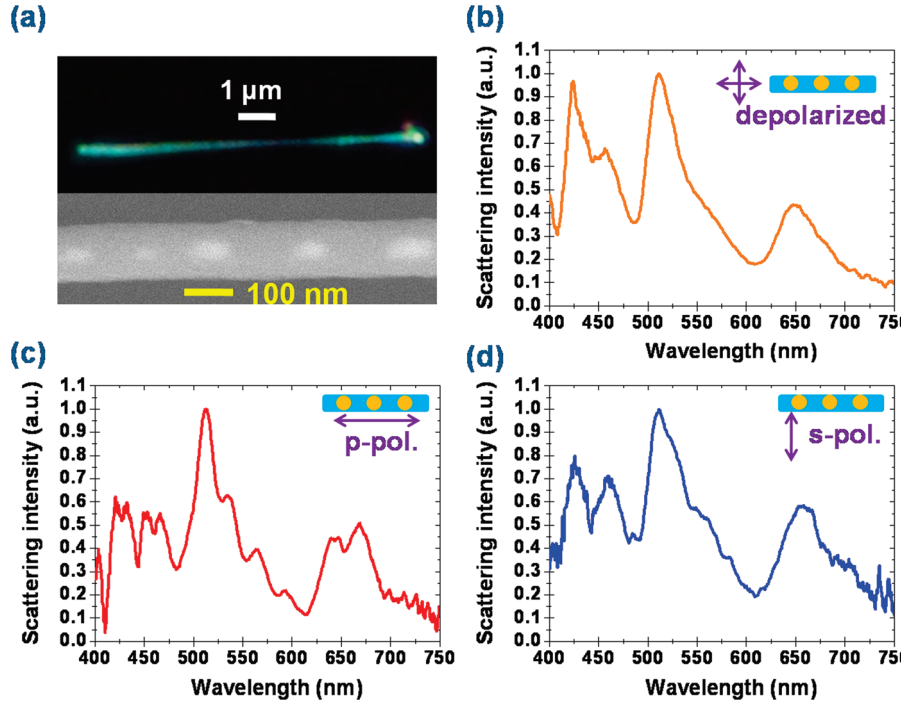

Figure 5. (a) The dark-field optical image and corresponding SEM image of a gold-in-Ga_2O_3 peapod nanowire on the SiO_2 substrate. The interparticle-distance of Au particles is 120 nm. (b) The scattering spectrum under depolarized white light. Different polarization directions of scattering light are shown (c) parallel to the long axis of the nanowire and the Au particle array and (d) perpendicular to it.

the size and morphology of Au peas, interparticle distance, and thickness of the dielectric layers. Agreement between the experimental results and calculations based on Mie and Gans theory verified the plasmonic properties of the Au nanostructures embedded in the Ga_2O_3 nanowires. Consequently, performance of gold-in-Ga_2O_3 nanophotonic devices can be predicted, realized, and optimized by carefully tuning experimental conditions in line with theoretical simulations. The observed modulation in the p-polarized spectrum revealed that the future vertical surface plasmon Fabry−Pérot resonators made by plasmonic nanocavity due to the short propagation length of surface plasmons can be realized and optimized.

EXPERIMENTAL SECTION

Synthesis and Characterization of Gold-in-Ga_2O_3 Nanowires. A horizontal furnace with three-zone controlling system was used to heat the quartz tube to 800 °C with a ramping rate of 20 °C /min; 0.3 g Ga (purity 99.9999%) metal powder and amorphous SiO_2 substrate were placed into the quartz furnace tube. Prior to the loading of Ga source and silica substrates into the furnace, an ordered monolayer of 488 nm polystyrene (PS) spheres was dispersed on the Si (100) substrate with a 350 nm SiO_2 capping layer. Subsequently, a 40 nm Au layer was deposited by electron beam evaporation process on the substrate with a monolayer of PS spheres. For microstructural analysis, the morphologies and crystal structures were characterized by field-emission scanning electron microscope (FESEM, JSM-6500F) and field-emission transmission electron microscope (FETEM, JEM-3000F), respectively. The FETEM is equipped with an energy dispersive spectrometer (EDS) and a Gatan GIF 2001 electron energy loss spectrometer (EELS) operated at 300 keV with a point-to-point resolution of 0.17 nm and was used to determine the crystal structures and chemical compositions.[30−33]

Light-Scattering Spectra Measurements. The plasmonic resonance of the gold-in-Ga_2O_3 peapod nanowires and gold-in-Ga_2O_3 core/shell nanowires was studied by far-field optical scattering spectroscopy. The optical images were obtained with an optical microscope (BX51, Olympus, Japan) with an objective of MPLFLN 100X, numerical aperture 0.90. All color optical images presented in the study were taken with the CCD camera attached to the microscope. Excitation light generated from a 100 W halogen lamp was focused and directed from above onto the sample by dark-field illumination through the objective. Backscattered light from the selected nanowire was then collected by the same objective and focused onto an image plane aperture that defined a 2 μm collection region on the sample, and finally directed into the fiber-coupled spectrometer (BTC111E, B&W TEK, U.S.A.). The scattering spectra obtained were further analyzed. Data processing including boxcar smoothing and intensity normalization was applied. The background signal from the silica substrate was subtracted from each spectrum presented in this study.

Acknowledgment. This work was financially supported by the National Science Council through Grant Nos. NSC 95-2221-E-007-245-MY2 and NSC 96-ET-7-007-002-ET. This work was also partially supported by Delta Electronics through Grant Nos. 98F2233EA and 97N2418E1.

Note added after ASAP publication: Due to a production error, the effective dielectric constant for Ga_2O_3 was incorrectly stated as n_{Ga_2}. The corrected version was published March 23, 2010.

Supporting Information Available: SEM images of the microstructures of the actual nanowires studied, the photoresponse behavior of a single gold-in-Ga_2O_3 peapod nanowire under periodic illumination by light of selected wavelengths, and the proposed mechanism for the observed interference fringes in the scattering spectrum of a single gold-in-Ga_2O_3 peapod nanowire. This material is available free of charge *via* the Internet at http://pubs.acs.org.

REFERENCES AND NOTES

1. McFarland, A. D.; Van Duyne, R. P. Single Silver Nanoparticles as Real-Time Optical Sensors with Zeptomole Sensitivity. *Nano Lett.* **2003**, *3*, 1057–1062.
2. Anker, J. N.; Hall, W. P.; Lyandres, O.; Shah, N. C.; Zhao, J.; Van Duyne, R. P. Biosening with Plasmonic Nanosensors. *Nat. Mater.* **2008**, *7*, 442–453.
3. Reinhard, B. M.; Siu, M.; Agarwal, H.; Alivisatos, A. P.; Liphartd, J. Calibration of Dynamic Molecular Rulers Based on Plasmon Coupling Between Gold Nanoparticles. *Nano Lett.* **2005**, *5*, 2246–2252.
4. Maier, S. A.; Kik, P. G.; Atwater, H. A.; Meltzer, S.; Harel, E.; Koel, B. E.; Requicha, A. A. G. Local Detection of Electromagnetic Energy Transport Below the Diffraction Limit in Metal Nanoparticle Plasmon Waveguides. *Nat. Mater.* **2003**, *2*, 229–232.
5. Lal, S.; Link, S.; Halas, N. J. Nano-Optics from Sensing to Waveguiding. *Nat. Photon.* **2007**, *1*, 641–648.
6. Oulton, R. F.; Sorger, V. J.; Pile, D. F. P.; Genov, D. A.; Zhang, X. A Hybrid Plasmonic Waveguide for Subwavelength Confinement and Long-Range Propagation. *Nat. Photon.* **2007**, *2*, 496–500.
7. Ozbay, E. Plasmonics: Merging Photonics and Electronics at Nanoscale Dimensions. *Science* **2006**, *311*, 189–193.
8. Hsieh, C.-H.; Chou, L.-J.; Lin, G.-R.; Bando, Y.; Golberg, D. Nanophotonic Switch: Gold-in-Ga_2O_3 Peapod Nanowires. *Nano Lett.* **2008**, *8*, 3081–3085.
9. Polman, A. Plasmonic Applied. *Science* **2008**, *322*, 868–869.
10. Barnes, W. L.; Dereux, A.; Ebbesen, T. W. Surface Plasmon Subwavelength Optics. *Nature* **2003**, *424*, 824–830.
11. Murray, W. A.; Barnes, W. L. Plasmonic Materials. *Adv. Mater.* **2007**, *19*, 3771–3782.
12. Maier, S. A. *Plasmonics, Fundamentals and Applications*; Springer: New York, 2007; pp 11−19, 39−52; 65−85.
13. Willets, K. A.; Van Duyne, R. P. Localized Surface Plasmon Resonance Spectroscopy and Sensing. *Annu. Rev. Phys. Chem.* **2007**, *58*, 267–297.
14. Quinten, M.; Leitner, A.; Krenn, J. R.; Aussenegg, F. R. Electromagnetic Energy Transport *via* Linear Chains of Silver Nanoparticles. *Opt. Lett.* **1998**, *23*, 1331–1333.
15. Rockstuhl, C.; Salt, M. G.; Herzig, H. P. Analyzing the Scattering Properties of Coupled Metallic Nanoparticles. *J. Opt. Soc. Am. A* **2004**, *21*, 1761–1768.
16. Rechberger, W.; Hohenau, A.; Leitner, A.; Krenn, J. R.; Lamprecht, B.; Aussenegg, F. R. Optical Properties of Two Interacting Gold Nanoparticles. *Opt. Commun.* **2003**, *220*, 137–141.
17. Su, K.-H.; Wei, Q.-H.; Zhang, X.; Mock, J. J.; Smith, D. R.; Schultz, S. Interparticle Coupling Effects on Plasmon Resonances of Nanogold Particles. *Nano Lett.* **2003**, *3*, 1087–1090.
18. Wei, Q.-H.; Su, K.-H.; Durant, S.; Zhang, X. Plasmon Resonance of Finite One-Dimensional Au Nanoparticle Chains. *Nano Lett.* **2004**, *4*, 1067–1071.
19. Qin, L.; Park, S.; Huang, L.; Mirkin, C. A. On-Wire Lithography. *Science* **2005**, *309*, 113–115.
20. Qin, L.; Zou, S.; Xue, C.; Atkinson, A.; Schatz, G. C.; Mirkin, C. A. Designing, Fabricating, and Imaging Raman Hot Spots. *Proc. Natl. Acad. Sci. U.S.A.* **2006**, *103*, 13300–13303.
21. Papavassiliou, G. C. Optical Properties of Small Inorganic and Organic Metal Particles. *Prog. Solid State Chem.* **1980**, *12*, 185–271.
22. Passlack, M.; Schubert, E. F.; Hobson, W. S.; Hong, M.; Moriya, N.; Chu, S. N. G.; Konstadinidis, K.; Mannaerts, J. P.;

Schnoes, M. L.; Zydzik, G. J. Ga_2O_3 Films for Electronic and Optoelectronic Applications. *J. Appl. Phys.* **1995**, *77*, 686–693.
23. Link, S.; El-Sayed, M. A. Spectral Properties and Relaxation Dynamics of Surface Plasmon Electronic Oscillations in Gold and Silver Nanodots and Nanorods. *J. Phys. Chem. B* **1999**, *103*, 8410–8426.
24. Link, S.; El-Sayed, M. A. Additions and Corrections. *J. Phys. Chem. B* **2005**, *109*, 10531–10532.
25. Johnson, P. B.; Christy, R. W. Optical Constants of Noble Metals. *Phy. Rev. B* **1972**, *6*, 4370–4379.
26. Ditlbacher, H.; Hohenau, A.; Wagner, D.; Kreibig, U.; Rogers, M.; Hofer, F.; Aussenegg, F. R.; Krenn, J. R. Silver Nanowires as Surface Plasmon Resonators. *Phy. Rev. Lett.* **2005**, *95*, 257403-1–257403-4.
27. Allione, M.; Temnov, V. V.; Fedutik, Y.; Woggon, U.; Artemyev, M. V. Surface Plasmon Mediated Interference Phenomena in Low-Q Silver Nanowire Cavities. *Nano Lett.* **2008**, *8*, 31–35.
28. Wiley, B. J.; Lipomi, D. J.; Bao, J.; Capasso, F.; Whitesides, G. M. Fabrication of Surface Plasmon Resonators by Nanoskiving Single-Crystalline Gold Microplates. *Nano Lett.* **2008**, *8*, 3023–3028.
29. Lyvers, D. P.; Moon, J.-M.; Kildishev, A. V.; Shalaev, V. M.; Wei, A. Gold Nanorod Arrays as Plasmonic Cavity Resonators. *ACS Nano* **2008**, *2*, 2569–2576.
30. Chueh, Y.-L.; Lai, M.-W.; Liang, J.-Q.; Chou, L.-J.; Wang, Z. L. Systematic Study of the Growth of Aligned Arrays of α-Fe_2O_3 and Fe_3O_4 Nanowires by a Vapor-Solid Process. *Adv. Funct. Mater.* **2006**, *16*, 2243–2251.
31. Chang, M.-T.; Chou, L.-J.; Chueh, Y.-L.; Lee, Y.-C.; Hsieh, C.-H.; Chen, C.-D.; Lan, Y.-W.; Chen, L.-J. Nitrogen-Doped Tungsten Oxide Nanowires: Low-Temperature Synthesis on Si, and Electrical, Optical, and Field-Emission Properties. *Small* **2007**, *3*, 658–664.
32. Chueh, Y.-L.; Hsieh, C.-H.; Chang, M.-T.; Chou, L.-J.; Lao, C. S.; Song, J. H.; Gan, J.-Y.; Wang, Z. L. RuO_2 Nanowires and RuO_2/TiO_2 Core/Shell Nanowires: From Synthesis to Mechanical, Optical, Electrical, and Photoconductive Properties. *Adv. Mater.* **2007**, *19*, 143–149.
33. Hsieh, C.-H.; Chang, M.-T.; Chien, Y.-J.; Chou, L.-J.; Chen, L.-J.; Chen, C.-D. Coaxial Metal-Oxide-Semiconductor (MOS) Au/Ga_2O_3/GaN Nanowires. *Nano Lett.* **2008**, *8*, 3288–3292.